Natural Resources Canada / Ressources naturelles Canada

GEOLOGICAL SURVEY OF CANADA
OPEN FILE 8861

Distribution of slope failures in eastern Baffin Island fiords, Nunavut

R. Bennett, A. Normandeau, and D.C. Campbell

2022

Canada

GEOLOGICAL SURVEY OF CANADA
OPEN FILE 8861

Distribution of slope failures in eastern Baffin Island fiords, Nunavut

R. Bennett, A. Normandeau, and D.C. Campbell

2022

Permanent link: https://doi.org/10.4095/329603

This publication is available for free download through GEOSCAN (https://geoscan.nrcan.gc.ca/).

Recommended citation
Bennett, R., Normandeau, A., and Campbell, D.C., 2022. Distribution of slope failures in eastern Baffin Island fiords, Nunavut; Geological Survey of Canada, Open File 8861, 1 .zip file. https://doi.org/10.4095/329603

Publications in this series have not been edited; they are released as submitted by the author.

1. Introduction

Submarine landslides, or slope failures, are a known hazard in Baffin Bay (Bennett et al., 2014; Broom et al., 2017; Brouard and Lajeunesse, 2019; Normandeau et al., 2021b). Recent studies have shown that slope failure activity appears to follow the retreat of glaciers in the area, meaning that active landslides are more likely to be present in the fiords of Baffin Bay rather than on the continental slope (Normandeau et al., 2020). Fiords are well-known to be more susceptible to submarine and subaerial sidewall failures, producing some of the largest tsunamis on Earth (Higman et al., 2018). Research over the last two decades has shown the presence of numerous slope failures in Baffin fiords, however there has been no systematic mapping of their deposits.

The purpose of this report is to identify and map slope failures in Eastern Baffin Island fiords (Figure 1). This was done by interpreting all existing multibeam echosounder and Huntec data that was of sufficient quality to observe these features. Databases were created that record a geographic position for each interpreted feature, as well as various observed characteristics and physical measurements that will be discussed later in this report. In addition to the identification of slope failures, the occurrence of seabed ice scour and sediment waves were also mapped at the same time. These features have implications for the distribution of slope failures as ice scours can trigger slope failures (Normandeau et al., 2021b) and sediment waves are an indicator of the presence of turbidity currents (Normandeau et al., 2019).

The intention is that this database will be used for further analysis of failures in Baffin Island fiords to improve the current understanding of their distribution, frequency, and potential triggers. Digital Geographic Information System (GIS) files containing information on all interpreted slope failures, sediment waves, and ice scours are included with this open file report. This research aims at helping to support Baffin Island communities and the Nunavut government in making decisions on public safety and the use of marine areas.

2. Background Geology

Fiords are deep estuaries located at high latitudes of both hemispheres that have been modified by the action of glacial ice. Canada has more fiords than the rest of the world combined, with over 50% of its fiords being located in the Canadian Arctic Archipelago (Syvitski et al., 1987). Baffin Island's eastern coastline is cut by fiords throughout the entire study area (Figure 1). It is speculated that fiords originated as river valleys (which themselves may follow pre-existing fault lines or other paths of least resistance) and then are further excavated by glacial ice (Syvitski et al., 1987). Most fiords contain one or more submarine sills that can give them unique sedimentological and oceanographic properties such as extreme (high or low) sedimentation rates or pronounced stratification of water properties.

Fiords could potentially contain as much as 24% of the total volume of marine sediment deposited in the last 100 ka (Syvitski et al., 1987). Limited sediment is generally deposited on steep fiord walls (i.e. where the slope is greater than the failure angle of the sediment, typically 5° to 30° depending on sediment type) but generally increases towards the centre, with ponding possible in deeper parts of the fiord. Inputs of sediment to high latitude fiords include glacial ice sources (supraglacial, englacial, and basal material), ice-rafted sources, fluvial sources, terrestrial sources, anthropogenic sources, and ocean sources (Syvitski et al., 1987).

Fiords are susceptible to slope failures due to their characteristic steep sides and potential for very high sedimentation rates. These conditions can lead to underconsolidated sediments lying on steep slopes that could fail under their own weight or be triggered by external factors (i.e. earthquakes, waves, delta progradation, or subaerial failures). New research shows that many fiords of Baffin Island are affected by submarine slope failures (Broom et al., 2017; Deering et al., 2019; Brouard and Lajeunesse, 2019; Normandeau et al., 2020) and that their triggers are likely different than lower latitude failures (Normandeau et al., 2021a, 2021b). Fiord sediments can also be highly variable due to the numerous input sources and diverse glacial histories. This sediment variability can lead to discontinuities and unconformities that may be potential failure surfaces (Syvitski et al., 1987). Many forms of mass transport process are believed to be active in fiords including rockfalls, slides, slumps, creep, debris flows, and turbidity currents (Syvitski et al., 1987). Significant subaerial (e.g. 2018 subaerial landslide in Karrak Fiord, Greenland) and submarine (e.g. Chenaga tsunami in Alaska; Brothers et al., 2016) slope failures are able to generate tsunamis in Arctic fiords.

Ice scours are extremely common features on the Baffin Shelf and in the Baffin Island fiords. Ice scour occurs when an iceberg or sea ice makes contact with the seabed and causes disturbance of sediments (Figure 2). There are two primary forms of ice scour, the first being a scour which is a linear feature (either straight or curved) formed when ice contacts the seabed and causes continual deformation as the ice is moved horizontally by wind, waves, or currents. The second type of ice scour is a scour pit which is a circular or slightly oblong depression caused when ice contacts the seabed and then remains in place until it is uncoupled from the bottom by melting and/or tidal action. Both ice scours and scour pits are observed on the Baffin Shelf and the Baffin Island fiords. Icebergs with keels up to 427 m deep have been observed in Baffin Bay (Milne, 1969) and up to 500 m in Labrador (Harris, 1974), eastern Greenland (Dowdeswell et al., 2007; Syvitski et al., 1996), and Antarctica (Barnes and Lien, 1988). The frequency of these extreme scour events are not known, but their implications are that any part of the Baffin Shelf could be impacted by ice scour. Fiords however are protected by their sills which regulate the size of iceberg that can enter each fiord. Icebergs with keel depths greater than the water depth at the fiord's sill will become grounded and likely returned to sea by wind and currents.

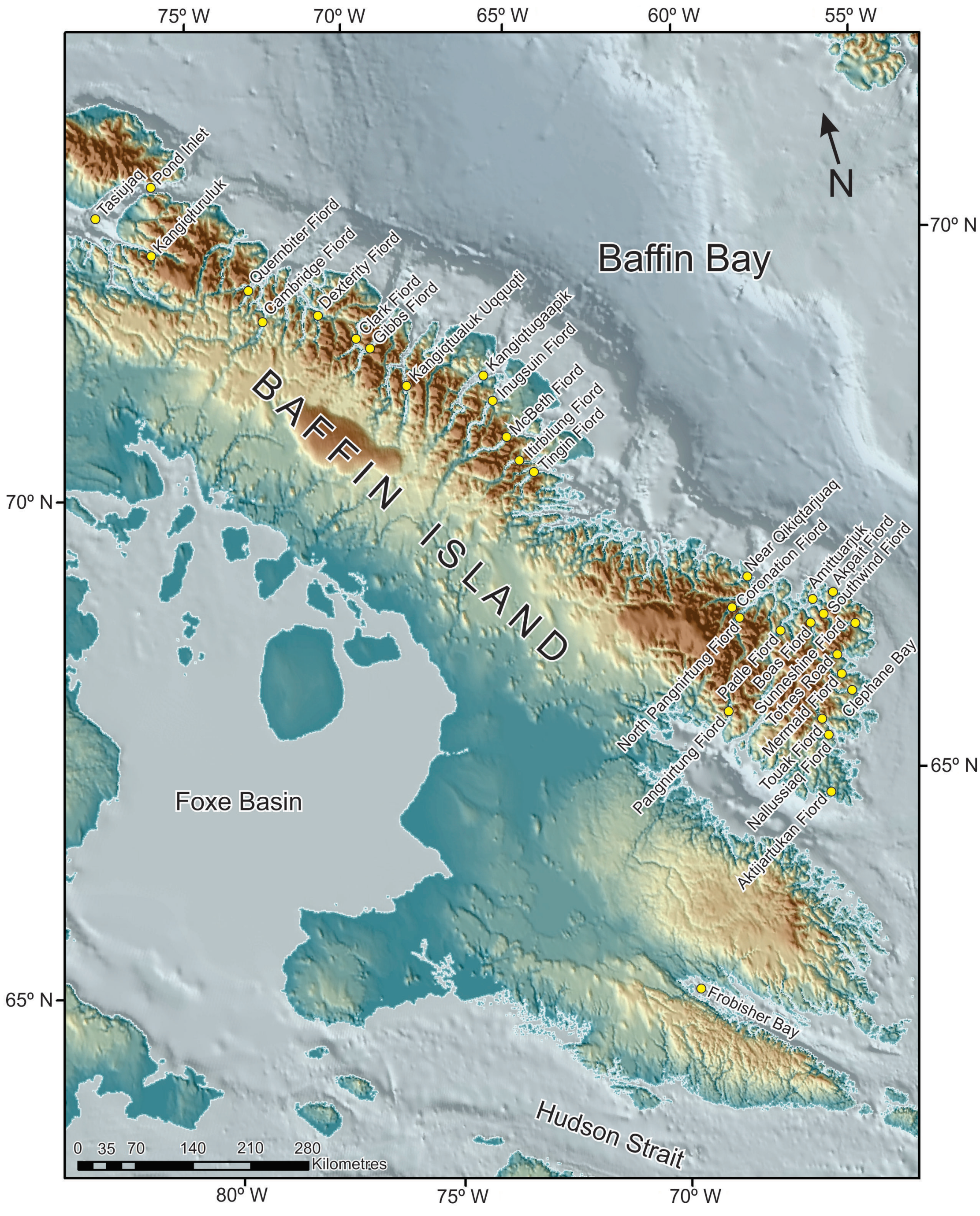

Figure 1: Location map.

3. Methods

A preliminary assessment of high-resolution geophysical data in the fiords of Baffin Island revealed that there were suitable multibeam, Huntec / 3.5 kHz sub-bottom profiler data available in a number of the fiords. These data were used to map slope failures, ice scours, and sediment waves with the results of this mapping being recorded in a database as described in this section.

3.1 Multibeam data

In order to map the distribution of slope failures in Baffin Island fiords, all available multibeam echosounder data were identified and assessed for quality. The multibeam data collected in the study area are from three sources: 1) the ArcticNet program onboard the CCGS Amundsen or the CSL Heron; 2) the Geological Survey of Canada (GSC) onboard the RV Nuliajuk and the CCGS Hudson; and 3) the Alfred Wegener Institute onboard the RV Maria S. Merian. All suitable data were then reprocessed to 2 m resolution and 4x vertical exaggeration if possible in the CARIS HIPS and SIPS software suite. This process provided data that was of sufficient quality to identify and measure slope failures, ice scours and sediment waves.

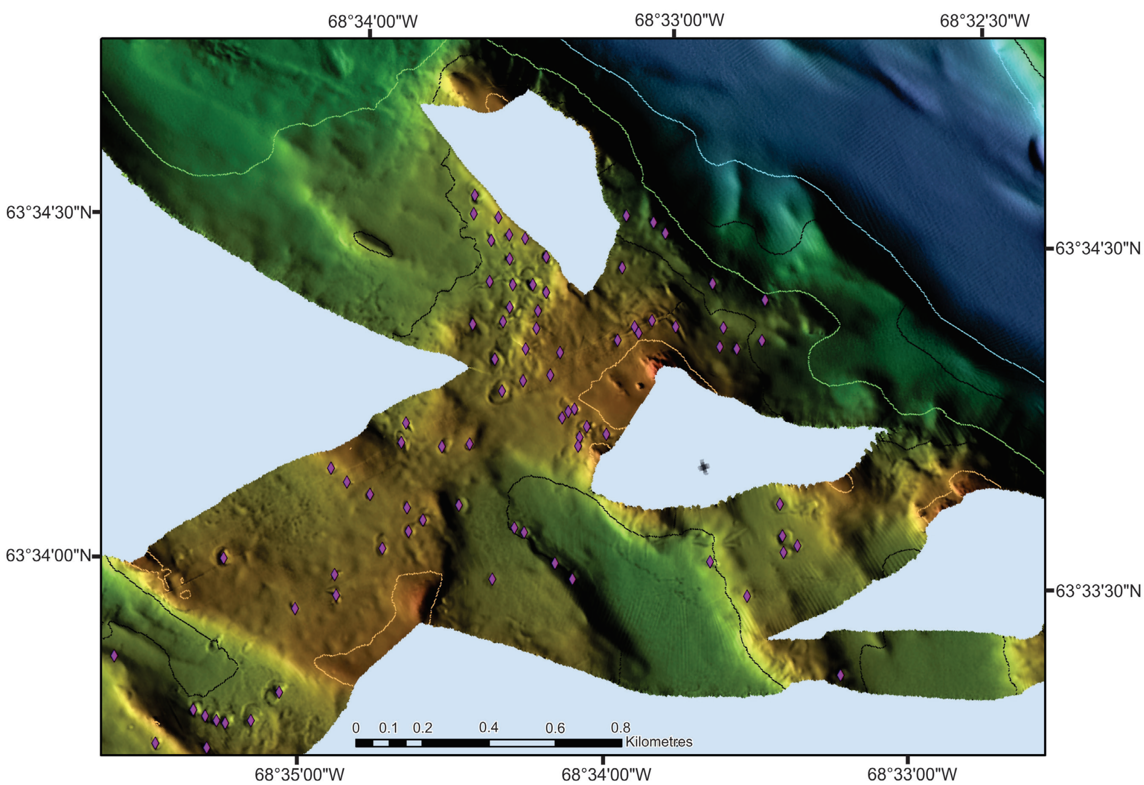

Figure 2: Ice scours on the seafloor of Frobisher Bay (marked by purple diamonds).

3.2 Huntec / 3.5 kHz sub-bottom profiler data

The Huntec Deep Towed System is a high resolution seismic reflection instrument used for imaging the upper ~50 m of sediment. It is towed beneath the sea surface to increase resolution and to decrease interference from vessel and wave noise. It is an excellent tool for imaging surface and near-surface slope failures. Huntec data from GSC cruise 82031 were re-examined for this to report as the data quality and coverage make it one of the best data sets for mapping the subsurface in the study area. Slope failures mapped by Broom et al. (2017) in Pond Inlet using 3.5 kHz sub-bottom profiler data from GSC cruise 2013029 were also included in the database.

3.3 Database structure

The multibeam data and the navigation information for the Huntec data were imported into a GIS. Three databases were created to better organize the interpreted features:

Database 1 – Slope failures: All seabed features interpreted as slope failures were mapped in the GIS, given a unique identification number, and measured / classified for seven parameters in a database as detailed later in this section. The data type, fiord name, and any comments from the interpreter were also recorded in the database.

Database 2 – Sediment Waves: Features identified as sediment waves were mapped in the GIS and given an identification number, classified for the morphology parameter (see below), and any comments by the interpreter were recorded. Sediment waves are an indicator of the presence of turbidity currents (Normandeau et al., 2019).

Database 3 – Ice Scours: Features identified as ice scours or pits were mapped in the GIS and given an identification number. There were no measurements or classifications done for the ice scours or pits.

The following information was recorded in the database for each slope failure.

<u>Id:</u> unique identifier number for each mapped slope failure

<u>Morphology:</u> interpretation of how well defined the feature is on geophysical records
wd = well defined
md = moderately defined
f = faint
b = buried (Huntec only)

<u>Type:</u> identifies if the feature is a single failure or a group of two or more failures (i.e. failure complex; after "Object type" in Clare et al., 2019)
s = single: a singular failure with one head scarp
m = multiple: a failure with more than one head scarp or a failure complex where multiple failures are attached to each other such that separate failures cannot be distinguished

Debris: denotes if a debris deposit is visible at the downslope termination of the feature
v = visible
nv = not visible

Rmax: maximum runout length, including debris field, of the failure in meters (see Figure 3; after "total length" in Clare et al., 2019). The maximum along track length of a slope failure mapped with Huntec data was recorded in the Rmax field. However, subsurface data does not provide orientation so it is not known if measurements from Huntec represent Rmax, Wmax or neither.

Wmax: maximum width, including debris field, of the failure in meters (see Figure 3; after "scar width" in Clare et al., 2019). Wmax values were not recorded for slope failures mapped using Huntec data as subsurface data cannot determine feature orientation (The maximum along track length of a slope failure mapped with Huntec data was recorded in the Rmax field).

Hmax: head scarp width in meters (see Figure 3). If head scarp is not visible, this value is 0 and "h/s not visible" will be included in the comments. Head scarp width is not measurable in Huntec data therefore this field is not applicable and the code 999 is used.

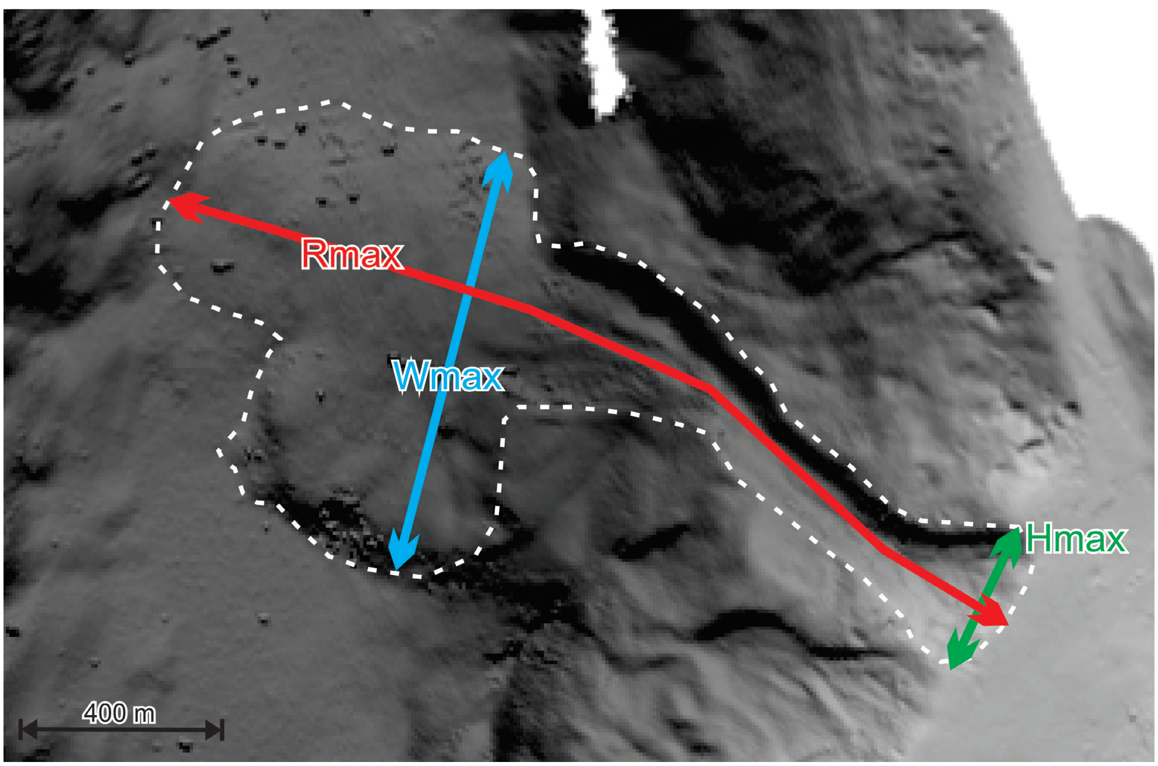

Figure 3: Example of measurements of Rmax (red), Wmax (blue), and Hmax (green). Slope failure outlined by dashed white line (ID# 57).

Scour: observations of ice scours near the head scarp of the failure (within ~300m).
y = yes

n = no
na = not applicable as the data coverage is not complete enough to observe ice scours and/or the head scarp is not visible

Fiord: name of the fiord where the feature is located

Source: source of the data used to make the interpretation

Comments: any comments by the interpreter

4. Results

Thirty-one fiord areas (see Figure 1 and Table 1) have been mapped to determine the occurrence of slope failures, sediment waves, and ice scours. Of these, 21 have been mapped using multibeam data only, 7 have been mapped using huntec data only and 3 were covered by both types of data. Table 1 details the fiords that have been mapped using multibeam echosounder or Huntec and if slope failures or sediment waves were observed at each location. Sediment waves cannot be determined from Huntec data alone so they were not included in the Huntec section of the table. Ice scours are visible in all fiords mapped with multibeam data.

Table 1 – List of fiords mapped during this study and identified features (see Figure 1 for fiord locations).

	Fiord	# Slope failures	# Sediment wave areas	# Ice Scours
Multibeam echosounder	Frobisher Bay	154	1	1525
	Pangnirtung Fiord	3	1	--
	Mermaid Fiord	5	1	862
	Totnes Road	--	2	596
	Akpait Fiord	2	5	318
	Southwind Fiord	57	2	205
	Boas Fiord	9	1	415
	near Qikiqtarjuaq	4	1	597
	Touak Fiord	--	2	838
	Nallussiaq Fiord	--	--	100
	Aktijartukan Fiord	--	--	22
	Clephane Bay	--	1	952
	Amittaurjuk	--	--	308
	Gibbs Fiord	4	--	--

	Clark Fiord (also mapped with Huntec, see below)	4	1	--
	Kangiqtualuk Uqquqti	--	--	32
	Quernbiter Fiord	--	--	--
	Dexterity Fiord	--	--	71
	Kangiqluruluk	1	4	11
	Padle Fiord	5	1	46
	Kangiqtugaapik	6	--	55
	Tasiujaq	1	3	383
	Pond Inlet (also mapped with 3.5 kHz sub-bottom profiler, see below)	--	--	99
	Coronation Fiord (also mapped with Huntec, see below)	1	1	--
Huntec / 3.5 kHz profiler	Sunneshine Fiord		n/a	n/a
	Coronation Fiord	3	n/a	n/a
	North Pangnirtung Fiord	4	n/a	n/a
	Tingin Fiord	4	n/a	n/a
	Itirbilung Fiord	6	n/a	n/a
	McBeth Fiord	6	n/a	n/a
	Inugsuin Fiord	6	n/a	n/a
	Clark Fiord	7	n/a	n/a
	Cambridge Fiord	5	n/a	n/a
	Pond Inlet	2	n/a	n/a

(-- = no occurrence; n/a = not applicable to this data type)

4.1 Slope failures and sediment waves

Slope failures are located in 77% of the fiords that were examined during this study. In total, 326 failures (299 slope failures and 27 turbidity current sites interpreted from sediment waves) were interpreted from the available multibeam echosounder and Huntec data (Figure 4). Slope failure distribution in the eastern Baffin Island fiords appears to be influenced by sediment thickness. The fiords that lack the presence of slope failures appear rocky with little to no sediment cover in multibeam echosounder data (i.e. Aktijartukan Fiord, Figure 5). This could mean that either no slope failures are occurring in these fiords because there is no sediment to fail; or that they are occurring but are too small to be visible in multibeam data due to the lack of sediments. There does not appear to be a relationship between the occurrence of slope failures and latitude.

The failures that were observed in the multibeam data are small when compared to those that are located on the continental margin with the maximum runout (RMax) of 3269 m (failure ID #280 in Eclipse Sound) and a maximum width (Wmax) of a single slope failure being 1277 m (Failure ID# 297 in Clark Fiord). Measurements on some of the multiple, overlapping failures are greater than these maximum values (the greatest Wmax value on a failure complex is 18,893 m). Measurements of slope failures using Huntec data can also be larger but subsurface data does not provide an indication of the orientation of the feature; therefore it is not known if the measurements from Huntec data represent Rmax, Wmax or an oblique angle to these dimensions. Features observed in Huntec could also be outburst flood deposits which would account for their greater dimensions compared to failures observed in multibeam data.

The morphology parameter is an evaluation of how well defined or “fresh” the failure appears in the multibeam or Huntec data. The first intention of this evaluation was to give an indication of the level of confidence as to whether the feature was indeed an actual slope failure. Features given a well defined (wd) designation are easily recognizable as slope failures with high confidence. Features with a faint (f) designation were difficult to recognize and there was some doubt if they were caused by slope failure or some other seabed process. Features designated as moderately defined (md) also have high confidence but do not appear as crisp or well defined as the "wd" failures. The second intention of this parameter is to provide an estimation of the age and/or magnitude of the features. It is likely that the failures designated as "wd" are younger or failed with more energy than the "md" and "f" features. Some features observed in the Huntec data are buried (b) by overlying sediments making them the oldest failures mapped during this study.

Some slope failures observed can partially overlap or even completely overprint on top of another slope failure. These scenarios are captured in the "type" parameter where slope failures are designated as single (s) or multiple (m) features. The purpose of this parameter was to capture multiple failures at the same geographic location or overlapping features that could not be distinguished from each other. Some areas observed in the fiords are completely covered by multiple failures (Figure 6). About 18% of all features were recognized as multiple failures. The presence of multiple attached or overlapping failures in one area are likely due to preconditioning factors such as sediment geotechnical properties that are conducive to failure (i.e. low shear strengths, underconsolidation) or repetitive trigger mechanisms (i.e. rapid sediment input, delta progradation).

Some failures that were mapped from multibeam echosounder data did not appear to have any accumulation of failed sediments at their terminus. The "debris" parameter was created to capture features that appear to be slope failures but are lacking evidence of downslope deposition of failed sediments (features that do not show failure deposits are designated as "nv" or not visible, see Methods section). Possible explanations for this scenario include the re-suspension and transport of sediments by currents or the burial of failure deposits by other processes (Figure 7).

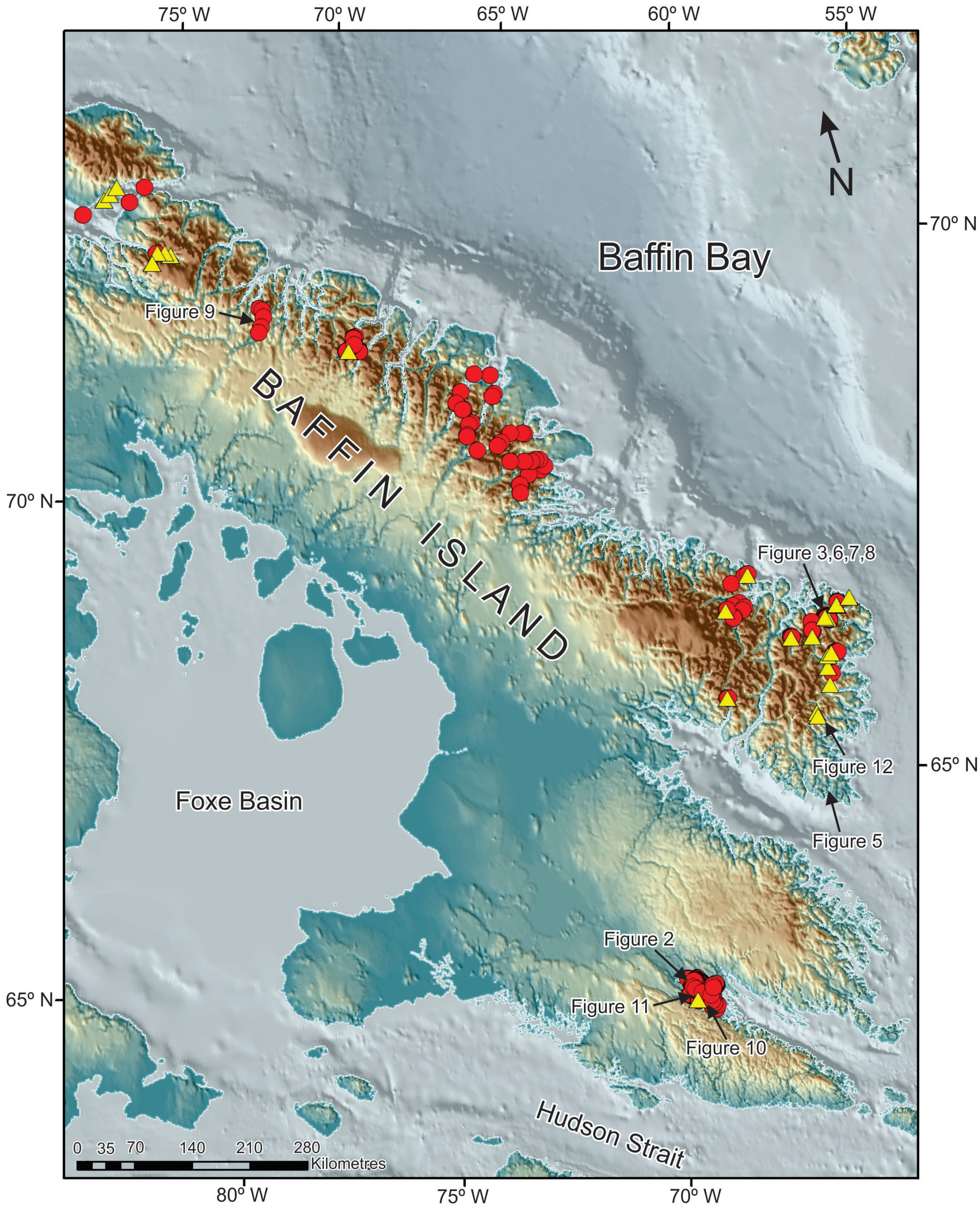

Figure 4: Distribution map of slope failures observed in Baffin Island fiords (red circles represent slope failures, yellow triangles represent turbidity currents interpreted from sediment waves).

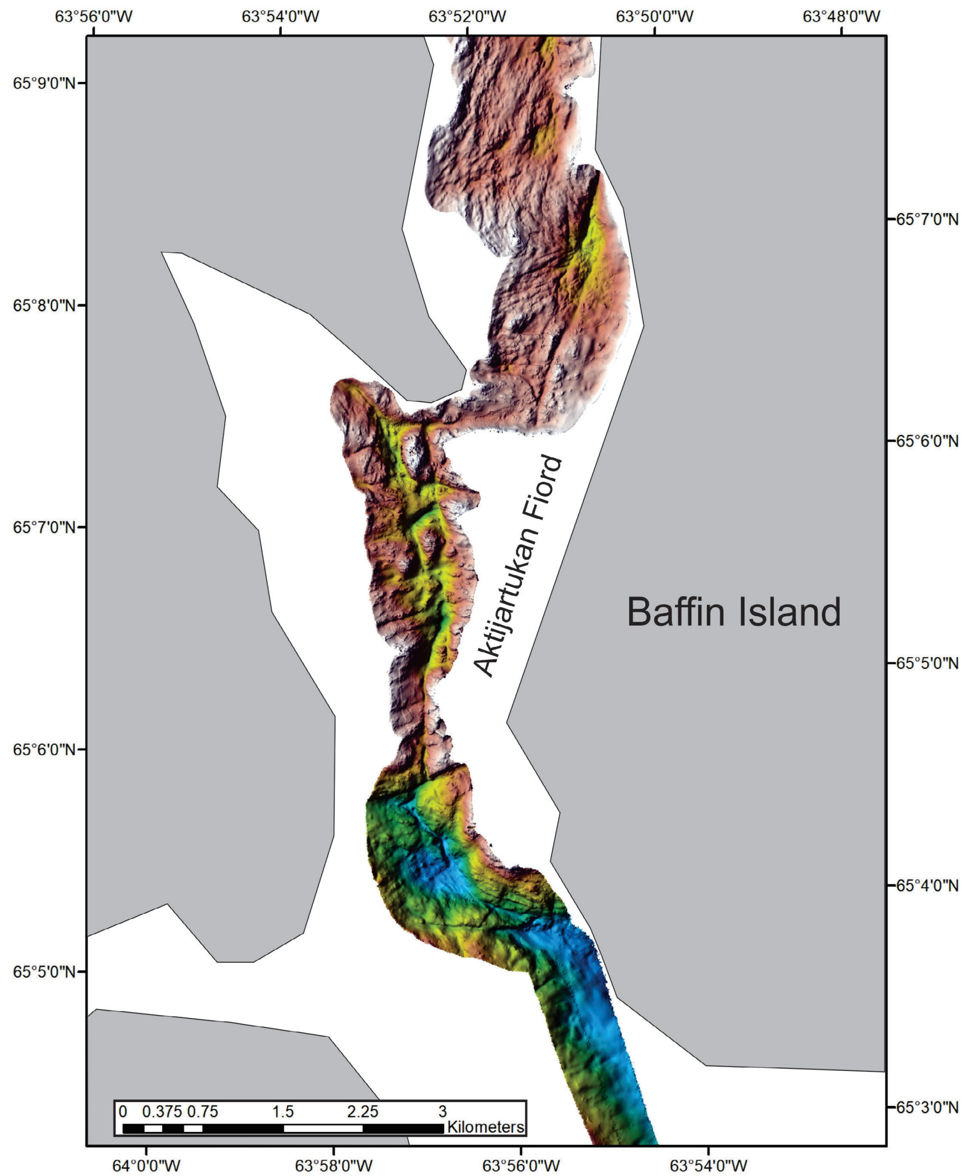

Figure 5: Rocky seafloor in Aktijartukan Fiord.

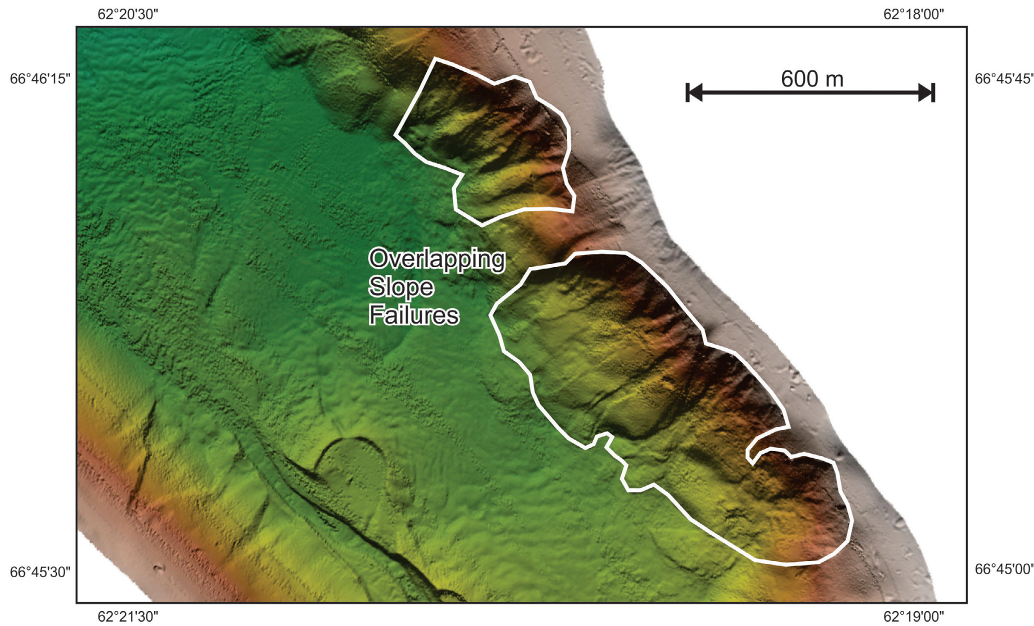

Figure 6: Overlapping slope failures in Southwind Fiord (ID# 12 – 18).

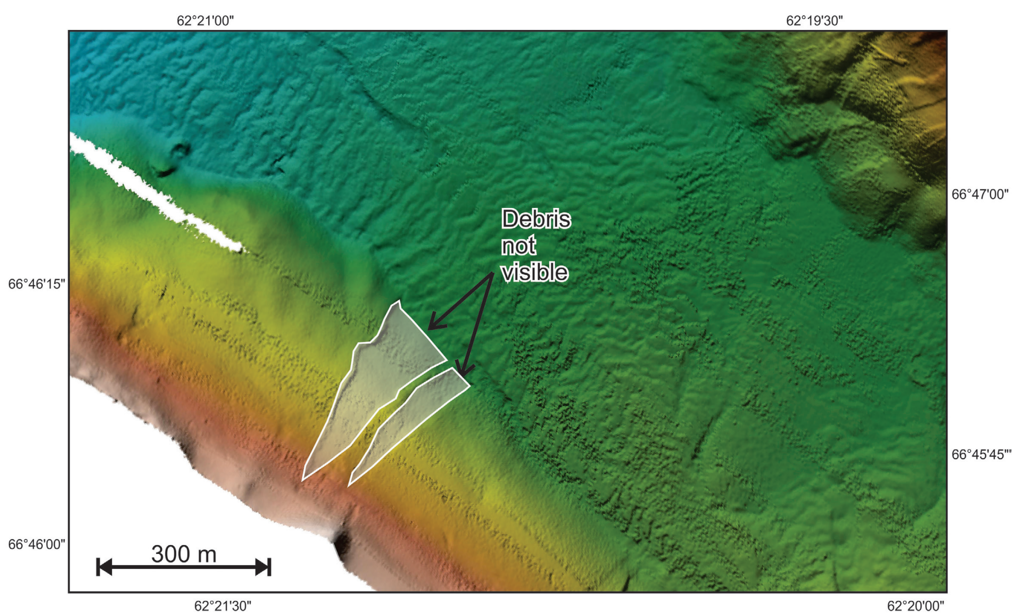

Figure 7: Two slope failures with no debris accumulation at their terminus in Southwind Fiord (ID# 1 and 2). The debris is likely covered by the sediment waves at the bottom of this fiord.

4.1.1 Types of failures

Several different styles of failures have been interpreted from the multibeam echosounder and Huntec data including slides, debris flows, and turbidity currents.

Slides

Slides are commonly observed in the Baffin Island fiords and are characterized by the rough or blocky texture of their debris fields (Figure 8). Most slides appear to be translational due to the smooth appearance of their failure surfaces such as in Figure 7, 8 and 9. A smaller number of slides show a rough, folded texture of their failure surface in multibeam echosounder data due to frontal thrusting (Figure 10). The slope failure in Figure 10 appears to have a headscarp and a sidescarp roughly perpendicular to each other. It is not clear if both of the headscarp and sidescarp were active contemporaneously or if failure from one created the conditions that lead to the creation of the other.

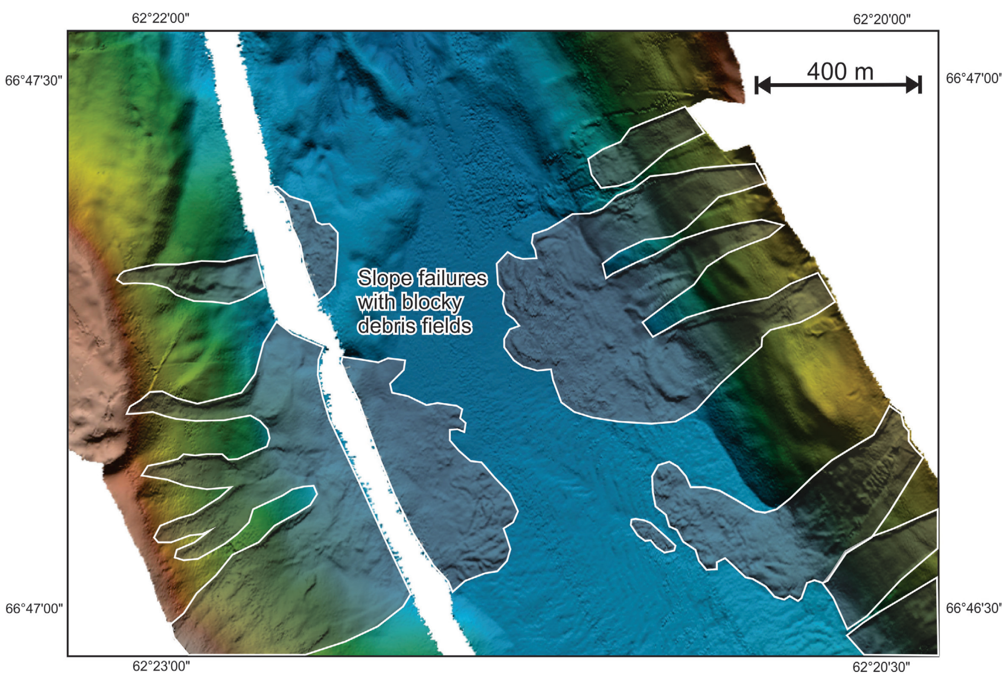

Figure 8: Slope failures in Southwind fiord with a rough blocky texture in their debris fields (ID# 36 – 40, 59 – 51).

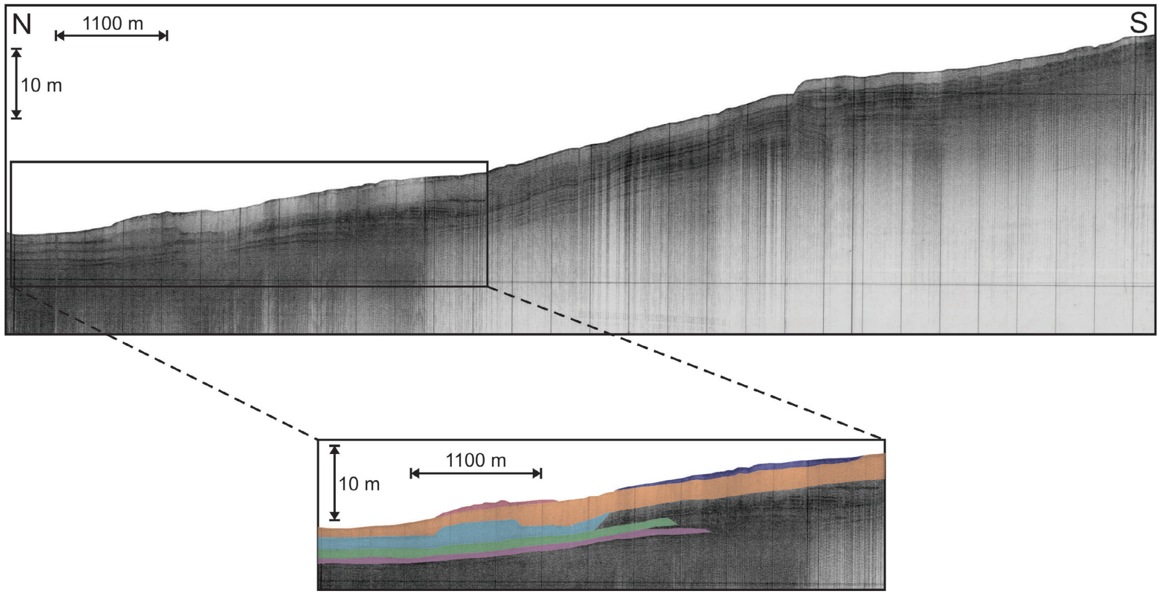

Figure 9: Stacked slope failures in Cambridge Fiord observed in Huntec data (ID# 113).

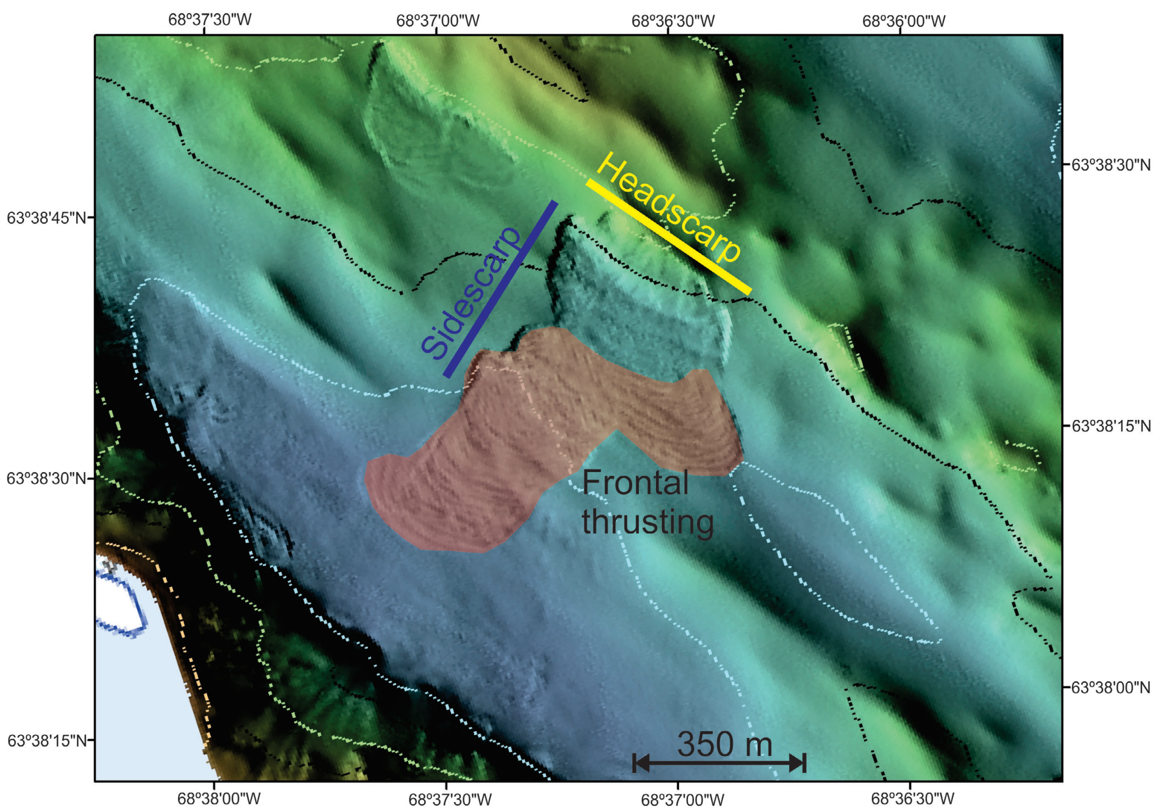

Figure 10: Slope failure from Frobisher Bay displaying characteristics of frontal thrusting in its lower section (ID# 125). This failure also appears to have a headscarp and a sidescarp.

Debris flows

Debris flows generally have higher water content and greater mobility than slide failures. In multibeam echosounder data, debris flows have a long run-out length, smooth texture of their debris fields, and are more likely to have a non-linear shape than slides. Figure 11 shows four slope failures that are interpreted to be debris flows located in Frobisher Bay. Each debris flow follows the contours of the seafloor to a deep basin where they terminate in a smooth, low-relief, terminal lobe. Debris flow 1 in Figure 11 is interpreted to be the oldest as it is overlain by debris flows 2 and 3. Debris flows 1, 2, and 3, are then truncated by the youngest debris flow, 4. Debris flow 4 occurred in two phases as the headscarp of 4a is no longer visible and was either overprinted by 4b or they originated from the same headscarp. Debris flow 4b is also observed incising into 4a. The sediments that comprise the terminal lobe are likely a mixture of material from all four debris flow events.

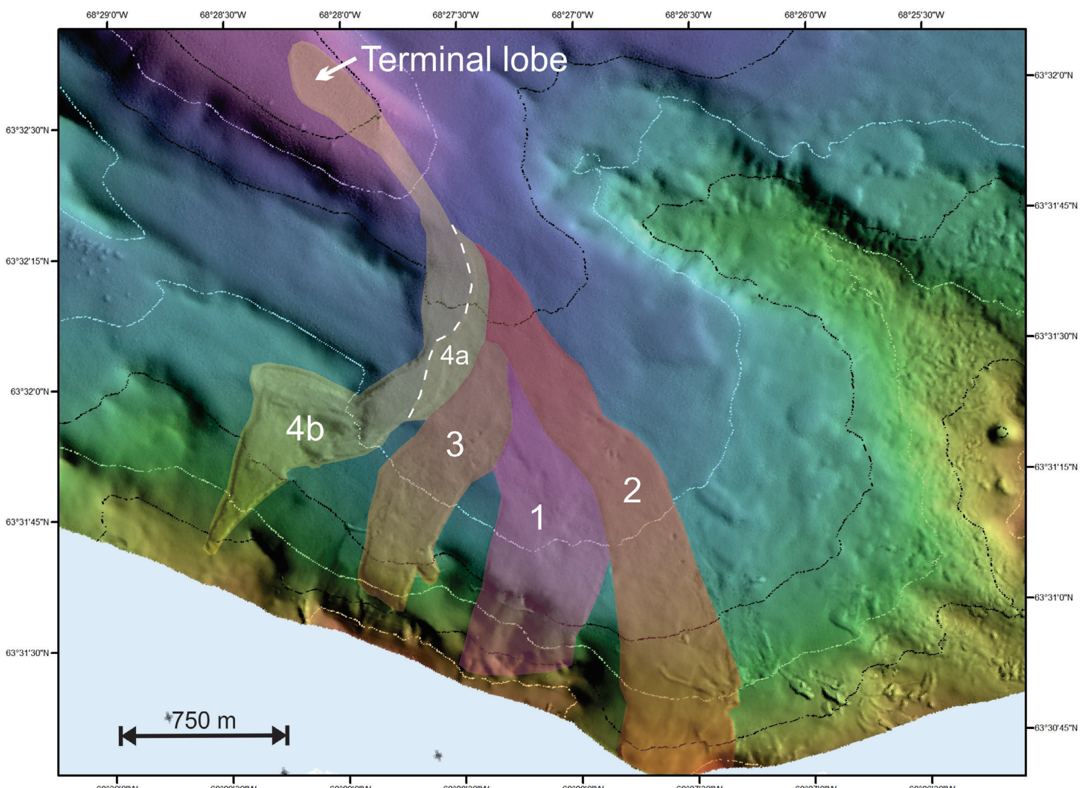

Figure 11: Multiple debris flows from Frobisher Bay depositing sediments in a small basin (ID# 166 – 170). Numbers show the order of deposition, 1 = oldest, 4 = youngest. Interpretation modified from Deering et al. (2019).

Turbidity currents

Turbidity currents are not directly observed in the Baffin Island fiords but are inferred from the presence of sediment waves in multibeam echosounder data (Figure 12).

Normandeau et al. (2019) showed that sediment waves on fiord deltas are due to recurring turbidity currents. Sediment waves were observed in multibeam data in about 43% of the fiords mapped during this study (see Table 1). Normandeau et al. (2019) also observed sediment waves in Kangiqłuruluk (formerly Oliver Sound). Seventeen of the twenty-seven instances of sediment waves observed (63%) are located on fiord head deltas. The occurrence of turbidity currents is low compared to slides and debris flows.

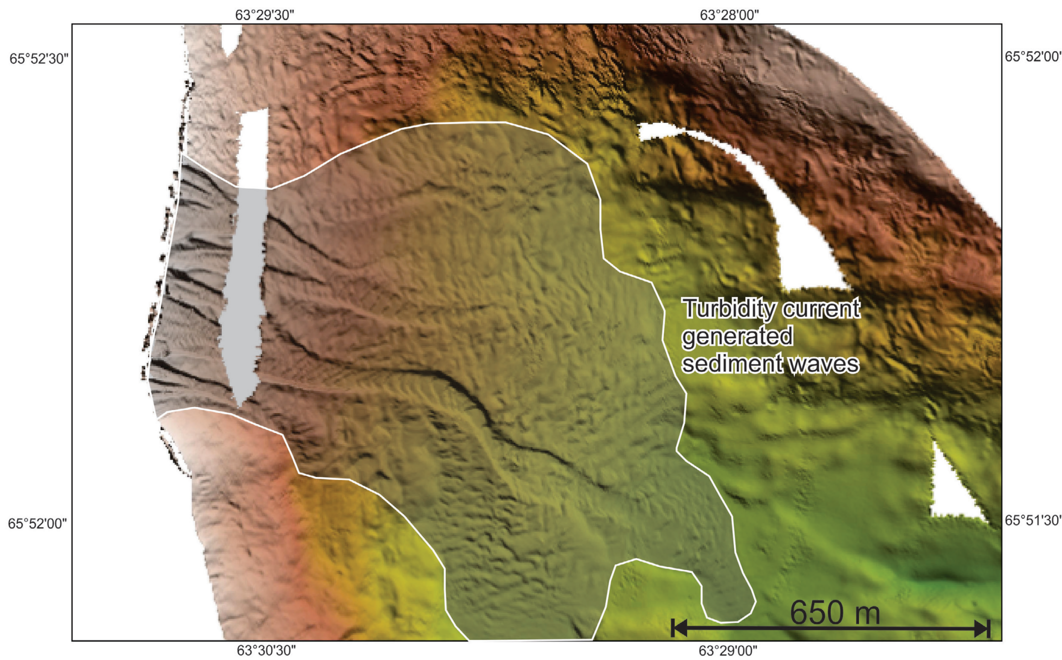

Figure 12: Sediment waves and channels in Touak Fiord caused by turbidity currents (ID# 12).

4.2 Ice scours

Ice scours are observed in 79% (19 of 24) of the fiords mapped with multibeam echosounder data (Figure 13). Most of the 7435 total scour features identified during this study are scour pits. Scour features are observed in water depths ranging from ~20 m up to ~115 m with the average water depth for all scours being about 50 m. The highest concentrations of scours are located on the slopes along the edges of the fiords as well as on ridges and mounds where the water shallows to water depths less than 100 m. From these results, it appears as though icebergs with keels greater than approximately 115 m rarely enter Baffin Bay fiords as they are likely blocked by sills at the mouths of the fiords.

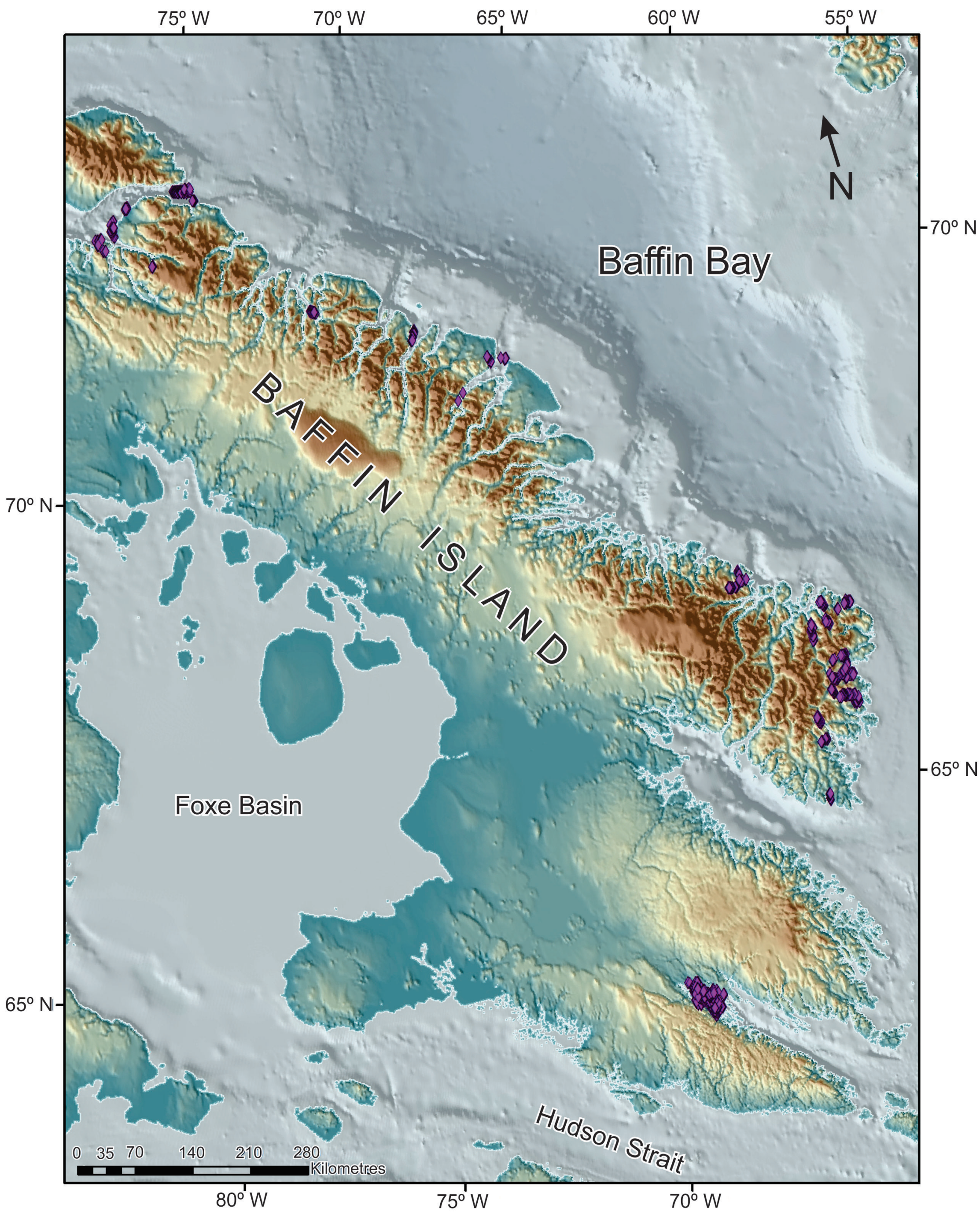

Figure 13: Distribution of ice scours observed in Baffin Island fiords (scours marked by purple diamonds).

New research by Normandeau et al. (2021b) shows that iceberg groundings can trigger submarine slope failures. The "scour" parameter in the database is meant to highlight sediment failures that show evidence of ice scours near their headscarp (within 300 m). It is possible that some of these features have been triggered by iceberg groundings but additional research would be required to make this determination.

5. Conclusion

After analyzing all available data in 31 eastern Baffin Island fiords, 77% (24 of 31) of the fiords show evidence of slope failures. The types of failures observed are slides, debris flows, and turbidity currents (inferred from sediment waves) with 326 features identified. Slides and debris flows are the most abundant failure types. Ice scours are observed in every fiord that was mapped with multibeam echosounder data.

Since slope failures are so widespread in eastern Baffin Island fiords, it is important that they are considered during seabed infrastructure projects or when making decisions regarding public safety and the environment.

5.1 Future Work

Detailed seafloor data that is sufficient for identifying slope failures does not exist in all Baffin Island fiords. Multibeam echosounder and/or high-resolution subsurface data (i.e Huntec) is required in these unmapped fiords to further improve our understanding of the characteristics and distribution of slope failures. Some fiords that were mapped for this study do not have complete multibeam data coverage so they require additional data collection to further refine the information presented in this report.

Additional sediment cores would be useful in determining failure mechanisms in Baffin Island fiords. Geotechnical analyses of these sediment cores would provide insight into the stability of fiord sediments and slope failure risk. Sediment cores would also help to determine the age and frequency of slope failures.

6. GIS digital files

This report is accompanied by GIS files that contain geographic positions, interpretations, and measurements (as described in the Methods section of this report) for all the slope failures, sediment waves, and ice scours mapped during this study. The files are names as follows:

Slope failures database = Baffin fiord failures.shp
Sediment waves database = Baffin fiord sed waves.shp
Ice scours database = Baffin fiord scour.shp

These GIS files are compatible with the software program ArcMap by ESRI. A free GIS data viewer is available from ESRI at http://www.esri.com/software/arcgis/explorer if required.

7. References

Barnes, P.W. and Lien, R. 1988. Icebergs rework shelf sediments to 500 m off Antarctica. Geology, v. 16, p. 1130-1133.

Broom, L.M., Campbell, D.C. and Gosse, J.C. 2017. Investigation of a Holocene marine sedimentary record from Pond Inlet, northern Baffin Island, Nunavut; in Summary of Activities 2017, Canada-Nunavut Geoscience Office, p. 93–104.

Brothers, D., Haeussler, P., Liberty, L., Finlayson, D., Geist, E., Labay, K. and Byerly, M. 2016. A submarine landslide source for the devastating 1964 Chenega tsunami, southern Alaska; Earth and Planetary Science Letters, 438. p. 112-121.

Brouard, E., Lajeunesse, P., 2019. Glacial to postglacial submarine landform assemblages in fiords of northeastern Baffin Island; Geomorphology, v. 330, p. 40-56.

Clare, M., Chaytor, J., Dabson, O., Gamboa, D., Georgiopoulou, A., Eady, H., Hunt, J., Jackson, C., Katz, O., Krastel, S., León, R., Micallef, A., Moernaut, J., Moriconi, R., Moscardelli, L., Mueller, C., Normandeau, A., Patacci, M., Steventon, M., Urlaub, M., Völker, D., Wood, L., Jobe, Z. 2019. A consistent global approach for the morphometric characterization of subaqueous landslides. Geological Society, London, Special Publications, 477, p. 455-477.

Deering, R., Bell, T., Forbes, D.L., Campbell, D.C., Edinger, E. 2019. Morphological characterization of submarine slope failures in a semi-enclosed fjord, Frobisher Bay, eastern Canadian Arctic. Geological Society, London, Special Publications, 477.

Dowdeswell, J.A., Ottesen, D., Rise, L. and Craig, J. 2007. Identification and preservation of landforms diagnostic of past ice-sheet activity on continental shelves from three-dimensional seismic evidence. Geology, v. 35, p. 359-362.

Harris, I. 1974. Iceberg marks on the Labrador shelf. In: Offshore Geology of Eastern Canada. B.R. Pelletier (ed.). Geological Survey of Canada, Paper 74-30, p. 97-101.

Higman, B., Shugar, D., Stark, C., Ekström, G., Koppes, M., Lynett, P., Dufresne, A., Haeussler, P., Geertsema, M., Gulick, S., Mattox, A., Venditti, J., Walton, M., McCall, N., Mckittrick, E., MacInnes, B., Bilderback, E., Tang, H., Willis, M., Richmond, B., Reece, R., Larsen, C., Olson, B., Capra, J., Ayca, A., Bloom, C., Williams, H., Bonno, D., Weiss, R., Keen, A., Skanavis, V., and Loso, M. 2018. The 2015 landslide and tsunami in Taan Fiord, Alaska. Scientific Reports, v. 8, 12993.

Milne, A., 1969. Underwater acoustics in ice-covered seas. Man in Cold Water Conference, Montreal, Quebec, May 1969, Oceanology Series no. 1, Department of Industry, Trade and Commerce, McGill University, p. 37-42.

Normandeau, A., Dietrich, P., Hughes-Clarke, J., Van Wychen, W., Lajeunesse, P., Burgess, D., Ghienne J-F. 2019. Retreat pattern of glaciers controls the occurrence of turbidity currents on high-latitude fjord deltas (eastern Baffin Island). Journal of Geophysical Research: Earth Surface, v. 124, no. 6, p. 1559 – 1571.

Normandeau, A., Campbell, D.C., Bennett, R., Macquarrie, M., MacKillop, K., Philibert, G., Sedore, P., Maselli, V., Jenner, K.A., 2020. Holocene and active marine geohazards in southeastern Baffin Island. Canada-Nunavut Geoscience Office, Summary of Activities 2019, Canada-Nunavut Geoscience Office, p. 93–100.

Normandeau, A., MacKillop, K., Macquarrie, M., Philibert, G., Bennett, R. 2021a. Southwind Fiord, Baffin Island, Nunavut: a natural laboratory to explore modern turbidity currents, submarine landslides and iceberg scouring in an Arctic environment. Summary of Activities 2020, Canada-Nunavut Geoscience Office, p. 81-92.

Normandeau, A., MacKillop, K., Macquarrie, M., Richards, C., Bourgault, D., Campbell, D.C., Maselli, V., Philibert, G., Hughes Clarke, J. 2021b. Submarine landslides triggered by iceberg collision with the seafloor. Nature Geoscience, 14, 599–605.

Syvitski, J., Burrell, D., Skei, J. 1987. Fjords: Processes and Products. Springer, London, 379 pp.

Syvitski, J.P.M., Stein, A. and Andrews, J.T. 1996. Icebergs and the sea floor of the East Greenland (Kangerlussuaq) continental margin. Arctic, Antarctic, and Alpine Research, v. 33, p. 52 – 61.